PUBLICATIONS OF THE ASTRONOMICAL SOCIETY OF THE PACIFIC, **115**:22–36, 2003 January

A Search for Cool Subdwarfs: Stellar Parameters for 134 Candidates[1]

DAVID YONG AND DAVID L. LAMBERT

Department of Astronomy, University of Texas, Austin, TX 78712; tofu@astro.as.utexas.edu, dll@astro.as.utexas.edu

Received 2002 September 3; accepted 2002 September 16; published 2002 December 4

ABSTRACT. The results of a search for cool subdwarfs are presented. Kinematic (U, V, and W) and stellar parameters ($T_{\rm eff}$, log g, [Fe/H], and ξ_t) are derived for 134 candidate subdwarfs based on high-resolution spectra. The observed stars span 4200 K $< T_{\rm eff} <$ 6400 K and $-2.70 <$ [Fe/H] < 0.25 including only eight giants (log g < 4.0). Of the sample, 100 stars have MgH bands present in their spectra. The targets were selected by their large reduced proper motion, by the offset from the solar-metallicity main sequence, or from the literature. We confirm the claims made by Ryan that the NLTT catalog is a rich source of subdwarfs and verify the success of the reduced proper-motion constraint in identifying metal-poor stars.

1. INTRODUCTION

The driving force behind our understanding of the chemical evolution of the Galaxy is the interpretation of observed abundance ratios. Self-consistent analyses of large high-quality data sets have revealed detailed abundance patterns (e.g., Edvardsson et al. 1993; McWilliam et al. 1995). Recent attempts to understand the observed abundance trends include endeavors by Timmes, Woosley, & Weaver (1995), Goswami & Prantzos (2000), and Alibés, Labay, & Canal (2001), who predict the evolution of the abundances of all elements from carbon through zinc. Cool stars provide a unique opportunity to test directly these models of Galactic chemical evolution through the abundances of low ionization potential trace elements (e.g., Rb, Cs) and isotopic ratios measured from molecular bands (e.g., Mg from MgH, Ti from TiO). Presently, these tests cannot be carried out because of the dearth of known cool metal-poor stars. In order to rectify this situation, we have commenced a search for cool subdwarfs, unevolved metal-poor stars that fall below the solar-metallicity main sequence in color-magnitude diagrams.

Searches undertaken by Carney & Latham (1987) and Ryan (1989) selected candidates drawn from proper-motion catalogs. These searches were successful in identifying metal-poor dwarfs for subsequent detailed abundance analysis. However, both searches neglected cool subdwarfs. An alternative to searches for metal-poor stars based on proper-motion catalogs is the objective prism surveys, which identify candidate metal-poor stars by the weakening of Ca II H and K. Such studies have been conducted by Bond (1970, 1980), Beers, Preston, & Shectman (1985, 1992), and others. Selection criteria that rely exclusively upon Ca features as metallicity indicators strongly bias the sample toward warmer stars. Since metal lines weaken with increasing $T_{\rm eff}$, a temperature estimate is required before deciding whether lines are abnormally weak. In the absence of temperature indicators, a cool metal-poor star will have Ca II features comparable to a warmer solar-metallicity star. More current work by Christlieb (2000) on the stellar content of the Hamburg/ESO Survey has dramatically increased the yields of metal-poor stars. Candidate metal-poor stars are identified from their location in ($B-V$)–Ca line strength space. By comparing the Ca line strength between stars of similar $T_{\rm eff}$, this increases the likelihood that a metal deficiency is the cause of the relative weakening of the Ca line in a candidate. With the remarkable success rate of 60% for stars below [Fe/H] $= -2.0$, twice as good as the HK survey by Beers and collaborators, we look forward to the results of the Hamburg/ESO Survey when applied to cool subdwarfs.

In this paper, we present the results of our search for cool subdwarfs, stellar ($T_{\rm eff}$, log g, [Fe/H], and ξ_t) and kinematic parameters (U, V, and W) for 134 stars. Our sample includes 80 stars with no prior metallicity estimates. In § 2, we outline and justify the selection criteria. The observations will be described in § 3 and the analysis in § 4. A discussion will be presented in § 5 and concluding remarks given in § 6.

2. SELECTION CRITERIA

Our goal was to find previously unidentified subdwarfs with 4000 K $< T_{\rm eff} <$ 4700 K and [Fe/H] < -1.5. We modeled our search upon the highly successful effort by Ryan (1989) using the New Luyten Two-Tenths (NLTT) catalog of stars with annual proper motions in excess of $0\farcs18$ yr^{-1} (Luyten 1979, 1980; Luyten & Hughes 1980). Subdwarfs are on plunging orbits, often highly elliptical, resulting in large transverse velocities relative to the local standard of rest (LSR). Subdwarfs are

[1] Based in part on observations obtained with the Hobby-Eberly Telescope, which is a joint project of the University of Texas at Austin, the Pennsylvania State University, Stanford University, Ludwig-Maximillians-Universität München, and Georg-August-Universität Göttingen.

therefore overrepresented in proper-motion catalogs. Following Ryan (1989), our primary criterion for ensuring that metal-poor candidates were selected was the reduced proper motion, $H = m_V + 5 \log \mu + 5$, where m_V is the apparent magnitude and μ is the proper motion in arcsec yr^{-1}. The reduced proper motion can also be expressed as $H = M_V + 5 \log \nu_T - 3.37$, where M_V is the absolute magnitude and ν_T is the transverse velocity in km s^{-1}. At a given spectral type, a reduced proper-motion constraint rejects stars whose transverse velocities fall below a chosen value. Subdwarfs are less luminous than disk dwarfs at a given color and have larger transverse velocities. Both effects conspire to increase the reduced proper motion of the subdwarf population relative to the disk dwarf population. We adopted Ryan's reduced proper-motion constraint requiring that stars have $H_R \geq 10.7 + 2(m_{pg} - m_R)$, where $H_R = m_R + 5 \log \mu + 5$ using Luyten magnitudes m_R and m_{pg}. We imposed a magnitude limit $m_R \leq 13.0$ and a declination limit $-40° \leq \delta \leq 90°$, as our observations were made at McDonald Observatory, where we required a reasonable signal-to-noise ratio (S/N) (60 pixel^{-1} at 6500 Å) in 20–30 minute exposures. To ensure that we observed cool stars, Luyten color classes $g-k$, k, and $k-m$ were selected. Carney & Latham (1987) and Ryan (1989) previously observed the $g-k$ color class. We included these stars so that we could compare our derived stellar parameters with the Carney and Ryan values. Ryan's photometry suggested that the color classes were not accurate. Stars assigned color class $g-k$ by Luyten actually span late F to late K. Further, the effect of the ultraviolet excess, the hallmark of a subdwarf, is to camouflage a cool subdwarf as a warmer disk dwarf in the Luyten color system. Altogether, our selection criteria resulted in 4445 NLTT candidate subdwarfs.

Our list was augmented by subdwarfs previously identified in the literature. Our final sources of candidate subdwarfs were color-magnitude diagrams constructed using the *Hipparcos* (ESA 1997) and Yale (van Altena, Lee, & Hoffleit 1995) parallaxes. Targets located beneath the solar-metallicity main sequence in the range $0.8 < B-V < 1.4$ were selected. Subdwarfs have a higher $T_{\rm eff}$ than disk dwarfs at a given mass, which shifts subdwarfs blueward of the disk main sequence. Reid et al. (2001) demonstrated that in the range $B-V < 0.8$, the majority of stars below the disk main sequence in a color-magnitude diagram based on *Hipparcos* data are not subdwarfs, [Fe/H] > -1.0. Errors in the colors cause these disk dwarfs to appear as subdwarfs. Our observations and analysis will test whether the Reid et al. (2001) findings are valid when we extend to cooler dwarfs, $0.8 < B-V < 1.4$. In total, we observed around 230 candidate subdwarfs, although in this paper we are reporting on 134 candidates.

3. OBSERVATIONS AND DATA REDUCTION

Table 1 contains the list of candidates observed at McDonald Observatory on the 2.7 m Harlan J. Smith telescope and on the 9.2 m Hobby-Eberly telescope (HET) between 1999 November and 2002 April. The 2.7 m data were obtained using the cross-dispersed echelle spectrometer (Tull et al. 1995) at the coudé f/32.5 focus with a resolving power of either 30,000 or 60,000. The detector was a Tektronix CCD with 24 μm^2 pixels in a 2048 × 2048 format. For this setting, the spectral coverage was from 3800 to 8900 Å with gaps between the orders beyond 5800 Å. The HET data were taken with the Upgraded Fiber Optic Echelle spectrograph (Harlow et al. 1996) at a resolving power of 11,000 on a 1024 × 1024 CCD. The spectral coverage was from 4500 to 9000 Å with gaps between the orders beyond 7300 Å. For observations on both telescopes, wavelength coverage incorporated the MgH A–X bands near 5140 Å as well as the TiO (0, 0) bandhead of the γ-system $A\,^3\Phi - X\,^3\Delta$ near 7054 Å. Visual inspection of the spectra readily indicated the presence or absence of the MgH or TiO molecular features (see Figs. 1 and 2). Of our sample of 134 stars, 34 displayed neither MgH nor TiO bands and 100 showed MgH or MgH and TiO bands. Numerous Fe I, Fe II, Ti I, and Ti II lines were available in the observed spectra for spectroscopic determination of stellar parameters. For each star, exposure times were generally 20–30 minutes and only occasionally were multiple exposures taken and co-added. Although varying from star to star, the typical S/N of the extracted one-dimensional spectra was 60 pixel^{-1} at 6500 Å. One-dimensional wavelength-calibrated normalized spectra were extracted in the standard way using the IRAF[2] package of programs. Equivalent widths (EWs) were measured using IRAF, where in general Gaussian profiles were fitted to the observed profile. Figure 3 shows the spectra of two different stars, one taken with $R = 60{,}000$ and the other at $R = 11{,}000$, where two Fe I lines used in the analysis are indicated. Although less than ideal, an equivalent width analysis of $R = 11{,}000$ spectra is feasible.

4. ANALYSIS

4.1. Deriving Stellar Parameters

The LTE stellar line analysis program MOOG (Sneden 1973) was used in combination with the adopted model atmosphere. For $\log g > 3.5$, we used the NEXTGEN model atmosphere grid for low-mass stars computed by Hauschildt, Allard, & Baron (1999). For giants with $\log g \leq 3.5$, we used LTE model atmospheres computed by Kurucz (1993). In both cases we interpolated within the grid when necessary. We derived the model parameters in the following way. We measured the equivalent widths of ~35 Fe I and around five Fe II lines. Values for $T_{\rm eff}$ were set from excitation equilibrium; $T_{\rm eff}$ was adjusted so that Fe abundances derived from individual lines were independent of excitation potential, as they must be. The Fe abundances derived from individual Fe I lines must be inde-

[2] IRAF is distributed by the National Optical Astronomy Observatory, which is operated by the Association of Universities for Research in Astronomy, Inc., under cooperative agreement with the National Science Foundation.

TABLE 1

BASIC DATA AND DERIVED PARAMETERS FOR OBJECTS

Name	R.A. (J2000.0)	Decl. (J2000.0)	Resolving Power[a]	$T_{\rm eff}$ (K)	[Fe/H]	log g (cm s^{-2})	ξ_t (km s^{-1})	$U_{\rm LSR}$ (km s^{-1})	σ_U (km s^{-1})	$V_{\rm LSR}$ (km s^{-1})	σ_V (km s^{-1})	$W_{\rm LSR}$ (km s^{-1})	σ_W (km s^{-1})	Luyten Color or Source	Molecular Features?
PLX 5805	00 01 55	26 00 15	30,000	4600	−1.72	4.25	1.0	120	10	−97	3	−26	8	Yale	Y
LP 524-64	00 08 00	08 16 42	30,000	4600	−1.04	5.00	1.0	−90	30	−95	25	8	13	$k-m$	Y
BD −14°142	00 48 22	−14 07 13	60,000	6200	−1.21	4.00	1.0	50	30	−225	110	2	25	$g-k$	N
LP 646-24	00 50 06	−04 26 00	30,000	4800	−1.01	4.50	0.7	−16	5	−120	45	−38	16	$g-k$	Y
G72-34	01 46 04	35 54 48	11,000	4800	−2.23	4.75	0.9	45	10	−265	165	−243	230	$g-k$	N
BD −4°290	01 52 18	−03 26 43	60,000	4900	−0.01	4.50	0.7	50	10	−2	1	−10	5	k	Y
BD +8°335	02 11 20	09 37 24	60,000	5100	−0.98	4.50	0.7	−35	2	−65	13	−54	5	$g-k$	Y
HIP 10412	02 14 11	01 33 12	30,000	4600	−0.40	4.75	1.2	−65	6	−24	5	2	3	Yale	Y
Cool 340	02 17 26	27 08 27	60,000	4800	−0.40	5.00	0.8	14	6	−98	17	16	7	$g-k$	Y
BD +4°415	02 34 35	05 26 47	60,000	4750	−0.63	4.50	0.6	122	6	−52	3	−15	6	k	Y
G78-26	03 16 27	38 05 56	30,000	4200	−1.01	4.75	0.6	65	5	−245	15	−17	6	Gizis97	Y
GJ 1064A	03 47 02	41 25 38	60,000	5000	−1.15	4.50	0.6	−106	3	−109	7	−71	4	FJ98	Y
GJ 1064B	03 47 03	41 25 42	60,000	4800	−1.15	4.50	0.6	−105	6	−130	17	−80	9	FJ98	Y
G175-7	03 48 28	51 14 06	11,000	5000	−1.76	4.00	1.0	−164	240	−515	400	−23	30	$g-k$	N
BD −4°680	03 51 54	−03 49 11	11,000	5800	−1.89	4.00	1.0	−232	40	−185	58	77	58	$g-k$	N
GL 158	04 03 15	35 16 24	60,000	4800	−1.79	5.00	1.0	−50	20	−185	4	26	1	FJ98	Y
G39-36	04 48 07	33 09 36	60,000	4200	−2.50	4.00	1.0	−14	8	−95	25	82	20	$g-k$	Y
G81-41	04 55 05	45 44 05	60,000	4550	−0.96	4.50	0.6	−8	4	−79	12	72	11	k	Y
BD −10°1085	05 04 22	−10 08 59	60,000	5100	−0.50	4.50	0.8	−6	3	−70	4	−27	1	$g-k$	Y
BD +19°869	05 12 53	19 43 20	60,000	4600	−1.01	4.50	0.5	0	1	−110	9	−5	1	k	Y
PLX 1219	05 23 10	33 11 30	30,000	4600	−1.79	4.00	0.6	−240	15	−125	90	9	5	Yale	Y
HIP 27928	05 54 34	−09 23 34	60,000	4200	−0.93	4.00	0.6	−70	3	25	3	45	4	Yale, HIP	Y
G103-27	06 16 48	29 57 06	60,000	5600	−0.95	4.50	0.6	0	5	−145	95	−118	80	K	N
G101-34	06 20 04	38 20 44	60,000	5000	−1.50	2.75	1.0	−336	374	−1425	4930	109	206	g[b]	N
HIP 30567	06 25 30	48 43 40	60,000	4700	−0.60	4.75	0.6	8	4	−104	12	−46	5	k	Y
G103-50	06 40 08	28 27 12	60,000	4700	−2.20	4.50	0.4	−147	38	−71	3	15	24	AAM96, CLLA94	Y
AC +78°2199	06 52 49	78 12 30	60,000	5000	−0.03	4.50	0.8	−120	19	−4	4	−114	23	$g-k$	Y
G88-1	06 58 28	18 59 49	60,000	4600	−0.84	5.00	1.0	2	3	−45	6	41	4	$g-k$	Y
BD −17°1716	06 59 29	−17 15 17	60,000	4600	−0.08	4.50	0.4	−53	3	44	3	−25	3	k	Y
G87-27	07 10 08	37 16 34	60,000	5100	−0.61	3.50	0.9	20	8	−230	76	−90	25	CLLA94	Y
G87-35	07 20 44	29 20 48	30,000	5300	−0.53	4.50	0.8	−51	5	−123	21	50	6	$g-k$	Y
G193-42	07 22 22	50 33 18	11,000	5000	−0.94	4.25	1.0	−155	35	−275	140	37	10	$g-k$	N
G193-49	07 27 22	52 26 12	30,000	5000	−0.39	5.00	0.9	−72	26	35	14	−118	58	k	Y
G90-4	07 30 23	27 16 18	11,000	5600	−0.81	4.50	1.0	7	10	−150	120	−108	80	$g-k$	N
GSC 03790−02030	07 45 34	56 57 22	30,000	5600	−1.16	4.00	0.7	−43	37	−84	50	−59	32	K	N
LP 208-60	08 21 44	38 47 13	11,000	5800	−0.22	4.00	1.0	50	35	−280	255	34	37	$g-k$	N
G115-1	08 22 17	41 04 24	30,000	4800	−1.33	4.50	0.6	−75	3	−84	23	34	4	$g-k$	Y
LP 545-17	08 25 40	05 15 28	11,000	5200	−1.01	4.75	1.0	52	105	−95	50	177	120	$k-m$	N
PLX 2019	08 29 41	01 44 48	30,000	4600	−1.72	4.50	1.0	237	101	−334	104	−11	14	Yale	Y
PLX 2023.01	08 30 00	−09 54 01	30,000	4400	−0.39	3.90	1.0	−12	1	4	1	10	1	Yale	Y
LP 209-14	08 31 10	42 13 48	11,000	5400	−1.36	4.75	1.0	−155	16	−270	265	92	15	K	N
G113-49	08 35 12	03 28 00	11,000	5100	−0.83	4.00	1.0	95	120	−180	110	77	35	$k-m$	N
G9-31	08 52 45	22 33 30	11,000	5600	−1.00	4.25	1.0	−96	16	−150	45	−93	45	$g-k$	N
LP 36-78	08 56 29	70 58 14	60,000	5150	0.25	4.50	0.7	−87	16	−56	23	31	2	k	Y
LP 786-61	09 05 14	−18 32 06	60,000	5800	−0.76	4.00	0.8	63	23	16	3	47	20	$g-k$	N
Ross 94	09 47 22	26 18 13	60,000	4600	0.00	3.50	1.0	−24	2	−49	8	−18	4	k	Y

TABLE 1 (*Continued*)

Name	R.A. (J2000.0)	Decl. (J2000.0)	Resolving Power[a]	$T_{\rm eff}$ (K)	[Fe/H]	log g (cm s^{-2})	ξ_t (km s^{-1})	$U_{\rm LSR}$ (km s^{-1})	σ_U (km s^{-1})	$V_{\rm LSR}$ (km s^{-1})	σ_V (km s^{-1})	$W_{\rm LSR}$ (km s^{-1})	σ_W (km s^{-1})	Luyten Color or Source	Molecular Features?
G116-55	09 48 19	34 07 12	30,000	5600	−2.10	4.00	1.0	−190	90	−165	130	−38	90	$g-k$	N
G43-7	09 50 13	05 09 05	30,000	4950	−1.02	4.50	0.8	113	19	−41	11	12	5	$g-k$	Y
G161-84	09 51 39	−03 50 00	60,000	4700	−1.31	4.75	0.4	−199	53	−96	17	131	15	CLLA94	Y
LP 788-55	09 54 33	−19 21 00	60,000	4700	−0.53	4.50	0.7	66	18	−4	6	−5	4	$g-k$	Y
Wolf 334	09 57 44	32 36 54	11,000	5200	−1.71	4.50	1.0	−450	320	−375	335	−163	300	$g-k$	N
LP 315-12	09 57 46	26 45 22	60,000	5100	−0.98	4.50	0.6	−122	15	−12	4	−14	11	$g-k$	Y
LP 429-17	10 01 08	14 18 42	60,000	4750	−0.10	4.50	0.4	47	10	−47	13	−15	3	$g-k$	Y
BD +53°1395	10 13 57	52 30 24	60,000	4500	−1.04	4.50	0.5	16	1	−79	3	12	1	k	Y
BD +12°2201	10 22 20	12 08 45	60,000	4500	−0.23	4.50	0.9	−57	3	−17	1	−9	2	k	Y
LP 790-19	10 26 07	−17 58 43	60,000	4300	−0.51	5.00	0.6	−111	7	−46	1	9	2	k	Y
BD −9°3104	10 35 29	−10 22 36	30,000	4900	−0.60	4.50	0.8	130	32	−82	14	−9	9	k	Y
G119-21	10 37 25	28 55 48	30,000	4600	−0.48	4.50	0.6	−81	24	58	15	−42	10	k	Y
BD +31°2175	10 40 16	30 48 55	60,000	4800	−0.17	4.75	1.1	−90	4	−35	2	−13	3	k	Y
PLX 2529.1	10 52 03	−00 09 38	60,000	4800	−0.58	4.50	0.5	39	3	−6	3	−52	2	Yale, HIP	Y
G119-45	10 57 21	30 59 48	30,000	4800	0.14	4.50	0.7	−177	39	−85	22	−53	20	k	Y
G58-36	11 03 13	22 00 24	30,000	4600	−0.05	4.50	0.8	−115	35	−47	15	15	16	k	Y
G253-46	11 08 06	82 24 54	60,000	5200	−0.57	4.50	0.7	0	2	−35	6	56	7	$g-k$	Y
BD −10°3216	11 11 11	−10 57 03	60,000	4500	−1.19	4.50	0.4	−122	3	−16	1	34	1	$k-m$	Y
HIP 55128	11 17 12	17 29 27	30,000	4900	−0.38	4.50	0.9	−124	26	−55	14	−53	12	k	Y
LP 792-12	11 18 58	−17 15 48	60,000	4800	−0.39	5.00	0.6	−77	14	−34	2	35	2	$g-k$	Y
BD +15°2325	11 22 19	14 26 44	60,000	4800	−0.58	4.50	0.6	−125	12	−46	5	−9	5	k	Y
G122-22	11 24 00	45 32 34	30,000	4400	−1.36	4.50	0.9	63	15	−36	8	58	8	k	Y
G163-80	11 25 07	−05 56 24	30,000	4700	0.05	4.75	0.6	−114	23	−55	9	0	8	k	Y
Ross 109	11 27 15	59 33 18	60,000	5300	−1.53	4.00	0.6	−350	300	−645	700	217	140	K	N
LP 733-14	11 38 29	−13 50 06	60,000	4700	−0.57	4.75	0.7	−15	3	−35	11	−41	10	$g-k$	Y
LP 734-54	11 57 54	−09 48 48	60,000	4800	−0.66	4.50	0.4	−78	13	−15	4	5	2	$g-k$	Y
Wolf 1424	12 00 19	20 35 43	60,000	4600	−1.19	4.50	0.4	−28	4	−120	25	−33	6	k	Y
LP 734-101	12 16 55	−11 49 06	60,000	5500	0.06	4.50	0.7	−86	16	−36	10	−9	4	$g-k$	Y
G13-29	12 19 20	02 26 42	30,000	4800	−0.66	4.50	0.6	−6	4	−101	30	−8	15	$g-k$	Y
G198-61	12 35 23	37 44 30	30,000	5300	−0.12	4.50	1.0	176	36	−42	11	21	7	k	Y
G149-9	12 48 03	27 45 48	30,000	4900	−0.62	4.75	0.8	24	16	−315	150	−86	1	k	Y
HIP 62627	12 49 56	71 11 39	60,000	4800	−0.24	5.00	1.2	−8	2	−93	3	−17	2	HIP	Y
G149-18	12 52 46	22 27 00	30,000	5000	−0.03	4.50	0.8	−214	44	−33	11	29	2	k	Y
W453	12 57 49	05 45 54	30,000	4600	−0.04	4.75	0.9	−71	17	−38	13	2	2	k	Y
HD 114095	13 08 26	−07 18 30	60,000	4730	−0.71	2.40	1.3	65	43	−290	166	−49	32	AAM96	Y
BD +68°714	13 10 21	67 29 41	30,000	4900	−0.05	4.50	1.0	−96	3	−70	2	7	1	K1	Y
Ross 466	13 15 14	−11 01 12	30,000	5000	−0.86	4.75	0.9	−71	17	−115	65	−103	30	$g-k$	Y
LHS 2715	13 18 57	−03 04 18	60,000	4400	−1.56	4.00	0.6	−40	7	−120	7	115	1	Gizis97	Y
LP 172-89	13 26 38	46 48 51	30,000	4800	−0.49	4.50	0.6	−124	28	−34	9	0	2	$g-k$	Y
LP 738-45	13 38 14	−15 47 14	30,000	4400	−0.12	4.50	0.8	−81	17	−28	14	14	4	k	Y
G255-44	13 55 36	74 00 12	60,000	4900	−1.30	4.50	0.7	−107	17	−25	15	74	7	k	Y
G65-22	14 01 44	08 55 17	60,000	5000	−1.66	4.50	0.4	10	8	−225	76	−83	25	AAM96, CLLA94	Y
BD +30°2490	14 11 24	30 05 02	30,000	4600	−0.18	4.75	0.6	−68	5	−88	8	35	3	k	Y
G239-12	14 18 53	73 14 12	60,000	5800	−2.62	4.00	1.0	74	25	−333	160	127	170	K	N
HIP 70152	14 21 14	08 58 16	60,000	4800	−0.05	5.00	1.0	50	7	−36	5	−20	4	RWMRKM01	Y
HIP 70715	14 27 45	23 50 27	60,000	4400	−0.11	4.50	0.6	−110	9	−66	6	−9	4	HIP	Y

TABLE 1 (*Continued*)

Name	R.A. (J2000.0)	Decl. (J2000.0)	Resolving Power[a]	$T_{\rm eff}$ (K)	[Fe/H]	log g (cm s^{-2})	ξ_t (km s^{-1})	$U_{\rm LSR}$ (km s^{-1})	σ_U (km s^{-1})	$V_{\rm LSR}$ (km s^{-1})	σ_V (km s^{-1})	$W_{\rm LSR}$ (km s^{-1})	σ_W (km s^{-1})	Luyten Color or Source	Molecular Features?
LP 500-92	14 34 13	12 34 57	30,000	4500	−0.38	4.50	0.9	−134	9	−37	4	10	5	$k-m$	Y
LP 175-8	14 36 10	45 08 59	30,000	4900	−0.31	4.75	0.6	−123	25	−65	14	33	10	k	Y
HD 131287	14 50 04	60 39 36	30,000	4800	−0.04	4.50	1.0	−4	1	−12	1	−13	1	k	Y
BD +23°2751	14 53 42	23 20 43	60,000	4700	−0.51	4.50	0.6	−76	2	−62	2	20	1	k	Y
LP 502-8	15 09 14	14 31 23	30,000	5000	−0.95	4.50	0.6	−80	17	−119	25	113	16	$g-k$	Y
HIP 74235	15 10 13	−16 22 46	60,000	4900	−1.51	4.50	0.8	295	2	−505	18	−62	10	HIP	Y
LP 802-56	15 19 12	−21 00 46	60,000	5200	−0.88	4.50	0.6	−143	7	−130	32	−82	7	k	Y
BD +2°2944	15 19 19	01 45 55	30,000	6000	−0.02	3.50	1.8	81	1	−8	1	−3	1	K4	N
Ross 804	15 45 29	−13 49 18	30,000	4600	−0.93	4.50	0.6	120	85	−285	360	−108	200	k	Y
G225-50	16 14 45	55 25 49	30,000	4600	−0.13	4.50	1.0	−60	13	−43	6	8	7	$g-k$	Y
LP 330-7	16 23 06	32 08 35	30,000	4800	−0.22	4.50	0.6	74	16	4	6	10	6	$g-k$	Y
G202-57	16 33 37	51 13 30	30,000	4900	−1.05	4.50	0.6	180	82	−65	32	49	18	$g-k$	Y
G17-25	16 34 42	−04 13 45	60,000	4950	−1.46	4.50	0.3	11	11	−115	24	−29	6	CLLA94	Y
BD −14°4454	16 36 14	−15 10 12	30,000	4600	−0.95	4.50	0.6	−111	2	−90	8	35	5	k	Y
LP 445-55	16 42 58	19 22 09	30,000	5200	−1.80	4.00	0.6	118	24	38	8	84	13	$g-k$	N
LP 447-2	17 08 05	17 57 38	30,000	5800	−1.79	4.00	0.9	−146	7	−272	26	46	18	$g-k$	N
LP 747-18	17 16 44	−13 01 12	30,000	5800	−0.95	4.50	0.8	71	51	−322	327	41	29	$g-k$	N
LP 447-34	17 17 08	18 07 06	30,000	4800	−0.35	4.50	0.9	53	18	−45	20	11	4	$g-k$	Y
G19-25	17 25 59	−02 44 36	60,000	4900	−2.01	4.50	0.4	116	86	−93	85	9	6	AAM96, CLLA94	Y
LP 808-11	17 33 53	−16 58 54	30,000	5500	−1.23	4.00	0.7	−35	40	−225	200	−78	65	$g-k$	N
BD −8°4501	17 47 28	−08 46 48	30,000	5800	−1.80	4.00	0.8	126	12	−45	16	−156	38	$g-k$	N
G204-47	18 09 29	47 13 24	30,000	5200	−0.88	4.50	1.0	170	126	−137	65	73	59	K	N
BD +5°3640	18 12 22	05 24 04	60,000	4950	−1.34	4.50	0.4	61	13	−216	21	38	5	AAM96	Y
BD −17°5287	18 40 57	−17 09 54	30,000	5800	−0.70	4.50	1.0	−60	25	−155	80	77	35	K	N
G227-44	18 41 43	58 34 30	30,000	5400	−1.45	4.50	1.0	−314	250	−210	11	−37	42	K	N
G207-23	19 16 13	37 04 20	30,000	5000	−1.90	4.00	0.6	−175	6	−319	1	41	15	K	N
HD 181007	19 19 28	−20 25 40	60,000	4700	−1.93	1.50	1.6	65	43	−290	166	−49	32	None[c]	N
LP 752-18	19 25 47	−11 09 54	30,000	5800	−1.00	4.00	1.0	60	25	−75	40	17	10	$g-k$	N
LP 753-29	19 50 04	−13 19 12	30,000	5400	−1.88	4.00	1.0	−65	26	−155	76	77	35	$g-k$	N
G23-14	19 51 50	05 36 46	60,000	5000	−1.51	3.00	1.0	116	86	−93	85	9	6	g[d]	N
LP 575-39	20 23 26	05 50 50	30,000	4700	−0.42	4.50	0.6	−90	13	−11	7	−19	12	$g-k$	Y
LP 575-40	20 23 56	05 24 44	30,000	4800	−0.10	4.50	1.0	−110	25	20	15	−29	18	$k-m$	Y
LP 815-43	20 38 14	−20 25 54	30,000	6400	−2.70	4.00	1.0	140	140	−290	265	36	27	$g-k$	N
HD 200968	21 07 10	−13 55 23	30,000	5000	−0.16	4.50	1.2	−52	1	−14	1	2	1	KF99	Y
BD +22°4567	22 10 31	22 47 49	30,000	4800	−0.33	4.75	1.1	75	4	−5	1	70	3	k	Y
BD +30°4633	22 12 06	31 33 41	60,000	4600	−0.01	4.50	0.8	92	6	−35	1	−6	2	$k-m$	Y
HIP 109801	22 14 24	−08 44 42	30,000	4600	−1.70	4.50	1.0	130	50	−225	75	−43	25	HIP	Y
Ross 237	22 53 30	27 45 18	30,000	4900	−1.49	4.25	0.9	−118	25	−315	16	8	25	k	Y
Ross 242	23 08 49	27 00 54	60,000	4700	−0.94	4.50	0.4	50	14	−130	16	−67	30	k	Y
LP 702-79	23 23 32	−06 00 12	30,000	4800	0.05	4.50	1.1	−150	60	−70	25	1	22	$g-k$	Y
HIP 115664	23 25 56	29 11 41	30,000	4600	−0.90	5.00	0.6	−85	16	−215	20	−78	25	HIP	Y
BD +28°4634	23 45 10	29 33 43	60,000	5000	−0.30	4.50	0.7	−138	3	6	2	−60	1	k	Y

NOTE.—Units of right ascension are hours, minutes, and seconds, and units of declination are degrees, arcminutes, and arcseconds.

[a] HET data taken with $R = 11{,}000$, 2.7 m data taken with $R = 30{,}000$ and 60,000.

[b] Star chosen from Carney et al. 1994 and Alonso et al. 1996a, but also in NLTT catalog.

[c] Star chosen from Alonso et al. 1996a; not in NLTT catalog.

[d] Star chosen from Carney et al. 1994, but also in NLTT catalog.

REFERENCES.—AAM96 = Alonso et al. 1996a; CLLA94 = Carney et al. 1994; FJ98 = Fuchs & Jahreiß 1998; KF99 = Kotoneva & Flynn 1999, private communication; Gizis97 = Gizis 1997; HIP = *Hipparcos* color-magnitude diagram; RWMRKM01 = Reid et al. 2001; Yale = Yale color-magnitude diagram.

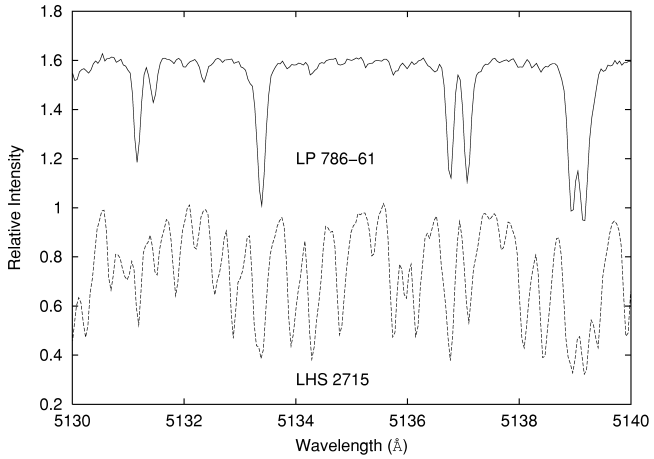

FIG. 1.—$R = 60{,}000$ data showing the absence (*top spectrum*) and presence (*bottom spectrum*) of the MgH A–X lines near 5140 Å. Many of the additional lines in the bottom spectrum are due to MgH.

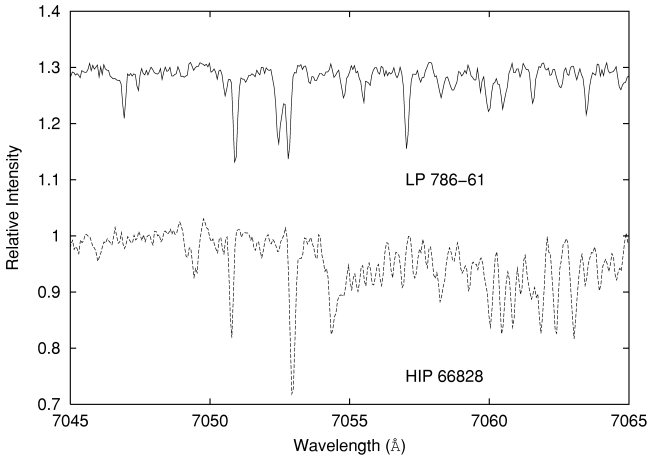

FIG. 2.—$R = 60{,}000$ data showing the absence (*top spectrum*) and presence (*bottom spectrum*) of the TiO γ-system $A\,^3\Phi - X\,^3\Delta$ bandhead near 7054 Å.

pendent of the strength of the line. Thus, the microturbulence ξ_t was estimated. Finally, the gravity was determined from ionization equilibrium. That is, the Fe abundance derived from Fe I lines must agree with the abundance derived from Fe II lines. This process was iterated until a consistent set of parameters were obtained (see Fig. 4). Ti I and Ti II lines were also used to check the stellar parameters. The final value of [Fe/H] was simply the weighted mean of the Fe I and Fe II abundances derived from the accepted model (see Table 1 for model parameters).

The *gf*-values of the Fe lines used in the analysis were selected from Lambert et al. (1996) and a list compiled by R. E. Luck (1993, private communication). The *gf*-values of the Ti lines were selected from the R. E. Luck compilation. Where possible, only weak lines, EWs < 90 mÅ, were used in the analysis. We checked our analysis techniques by observing

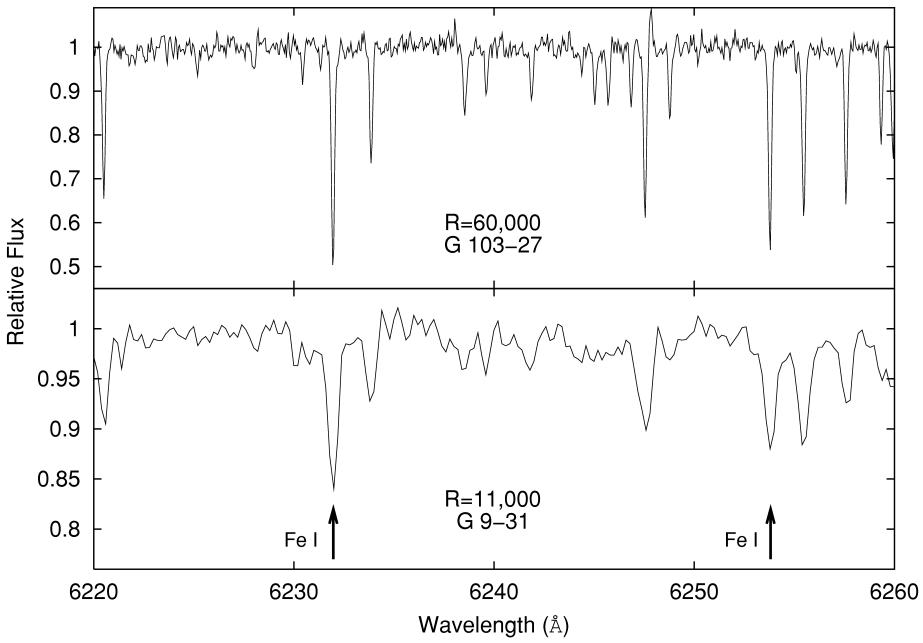

FIG. 3.—Spectra of G103-27 taken at $R = 60{,}000$ and G9-31 taken at $R = 11{,}000$. Both stars have similar stellar parameters. Representative Fe I lines used to derive stellar parameters are highlighted. Importantly, the $R = 11{,}000$ spectrum has Fe I lines for which equivalent widths can be measured.

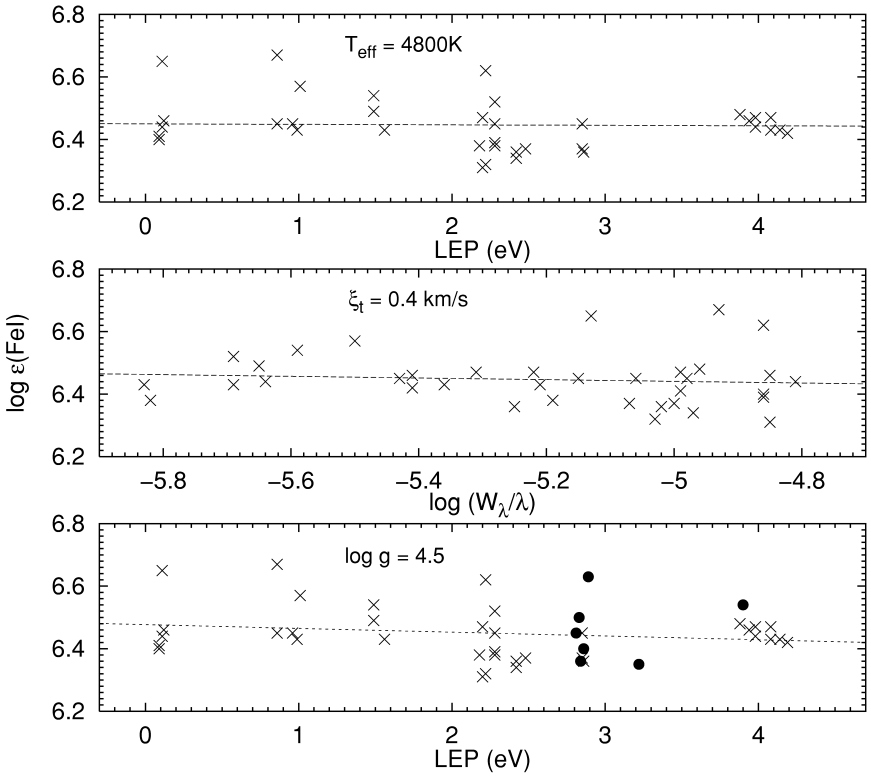

FIG. 4.—Determination of stellar parameters $T_{\rm eff}$, $\log g$, and ξ_t using excitation and ionization equilibrium for GJ 1064B. In the top panel, the lower excitation potential (LEP)-abundance relation is used to set $T_{\rm eff}$. In the middle panel, the reduced equivalent width (W_λ/λ)-abundance relation is used to determine ξ_t. In the bottom panel, the abundances of Fe I (*crosses*) and Fe II (*filled circles*) are used to fix $\log g$. In all panels, the line represents the least-squares fit to the data.

the solar spectrum at $R = 60{,}000$. We measured 30 Fe I lines and seven Fe II lines and compared our equivalent widths with the Grevesse & Sauval (1999) values. Our equivalent widths were larger by a mean value of 3.7 mÅ with a standard deviation of 2.6 mÅ. Using our equivalent widths and a NEXTGEN model atmosphere, we derived a solar abundance of $\log \epsilon(\mathrm{Fe}) = 7.54$. Considering the Grevesse & Sauval (1999) value of $\log \epsilon(\mathrm{Fe}) = 7.50 \pm 0.05$ derived from their empirical model solar atmosphere, we adopted $\log \epsilon(\mathrm{Fe}) = 7.52$ as the solar Fe abundance for this study.

Our derived model parameters, $T_{\rm eff}$, $\log g$, ξ_t, and [Fe/H], have associated uncertainties. We varied $T_{\rm eff}$ until the trends between lower excitation potential and abundance were unacceptable. Similarly, we took values for ξ_t that noticeably changed the trends between equivalent width and abundance. For $\log g$, we measured the standard deviation of the Fe abundance as derived from Fe I lines (typically 0.1–0.15 dex) and then allowed Fe I and Fe II to agree within this standard deviation. This produced uncertainties of $\delta T_{\rm eff} = 150$ K, $\delta \log g = 0.3$ dex, $\delta\xi_t = 0.3$ km s^{-1}, and δ[Fe/H] = 0.2 dex in the model parameters.

4.2. Comparison with Literature

For the 134 candidate subdwarfs analyzed here, a search on SIMBAD indicated that there were 37 stars with previously determined values for $T_{\rm eff}$ and 54 stars with previously determined values for [Fe/H]. We have compared our values with those found in the literature (see Table 2 and Figs. 5 and 6). We find a mean offset $\langle T_{\rm eff}$ (this study) $- T_{\rm eff}$(literature)$\rangle = -25$ K with a standard deviation of 114K. For [Fe/H], the mean offset is $\langle$[Fe/H](this study) $-$ [Fe/H](literature)$\rangle = -0.1$ dex with a standard deviation of 0.38 dex. The agreement is reasonable between the stellar parameters derived in this study and the values found in a variety of sources in the literature.

Table 2 shows values for [Fe/H] given by Ryan & Norris (1991) for a number of stars. However, these metallicities are not paired with values for $T_{\rm eff}$. The Ryan & Norris (1991) sample are reobservations of a subset of metal-weak stars identified in Ryan (1989). An index measuring the strength of the Ca II K line was calibrated empirically as a function of $B-V$ to give [Fe/H]. Alonso, Arribas, & Martínez-Roger (1996a, 1999a) determined $T_{\rm eff}$ using the infrared flux method, which

TABLE 2
COMPARISON WITH LITERATURE

	THIS STUDY		LITERATURE		
STAR	$T_{\rm eff}$	[Fe/H]	$T_{\rm eff}$	[Fe/H]	SOURCE
PLX 5805	4600	−1.72	…	−1.28	SPC93
LP 646-24	4800	−1.01	…	−0.24	RN91
G72-34	4800	−2.23	4689	−2.21	CLLA94
BD +8°335	5100	−0.98	5224	−0.80	CLLA94
	5100	−0.98	…	−0.61	Eggen98
BD +4°415	4750	−0.63	4756	−0.41	AAM96
	4750	−0.63	…	−0.43	Reid01
	4750	−0.63	…	−0.39	Eggen98
G78-26	4200	−1.01	…	−1.20	Gizis97
GJ 1064A	5000	−1.15	5049	−1.02	CLLA94
	5000	−1.15	5200	−1.05	TL99
	5000	−1.15	…	−0.85	TI99
	5000	−1.15	5050	−0.80	Fulbright00
GJ 1064B	4800	−1.15	4950	−1.11	TL99
	4800	−1.15	4816	−1.05	CLLA94
	4800	−1.15	…	−0.86	TI99
BD −4°680	5800	−1.89	5866	−2.07	AAM96
GL 158	4800	−1.79	4762	−1.73	CLLA94
	4800	−1.79	4700	−1.70	Fulbright00
	4800	−1.79	…	−1.67	TI99
	4800	−1.79	4775	−1.81	TL99
BD +19°869	4600	−1.01	…	−0.55	Eggen87
	4600	−1.01	…	−0.60	Norris86
PLX 1219	4600	−1.79	4935	−1.02	CLLA94
	4600	−1.79	…	−2.00	Morrison01
	4600	−1.79	4739	−1.61	AAM96
G103-27	5600	−0.95	5449	−0.93	SPC93
G101-34	5000	−1.50	5289	−1.83	AAM96[a]
	5000	−1.50	4955	−1.88	CLLA94
G103-50	4700	−2.20	4642	−2.00	CLLA94
	4700	−2.20	4713	−3.00	AAM96
G88-1	4600	−0.84	…	−0.13	RN91
	4600	−0.84	…	−0.40	SPC93
G87-27	5100	−0.61	4905	−1.45	CLLA94[a]
	5100	−0.61	5090	−0.42	GL00
G87-35	5300	−0.53	5222	−0.48	CLLA94
	5300	−0.53	…	−0.55	Eggen98
G90-4	5600	−0.81	5513	−0.86	CLLA94
PLX 2019	4600	−1.72	4740	−1.13	AAM96
G113-49	5100	−0.83	5194	−0.78	CLLA94
G9-31	5600	−1.00	5546	−0.94	CLLA94
	5600	−1.00	5569	−0.85	AAM96
G43-7	4950	−1.02	5009	−0.68	CLLA94
	4950	−1.02	…	−0.68	Reid01
G161-84	4700	−1.31	4650	−1.71	CLLA94
	4700	−1.31	…	−1.57	Beers99
Wolf 334	5200	−1.71	5084	−1.82	CLLA94
LP 792-12	4800	−0.39	…	0.18	RN91
G13-29	4800	−0.66	…	0.04	RN91
HD 114095	4730	−0.71	4650	−0.60	Fulbright00
	4730	−0.71	4541	−1.58	AAM96[a]
	4730	−0.71	4680	−0.35	Clementini99
BD +68°714	4900	−0.05	…	−0.17	Eggen98
LHS 2715	4400	−1.56	4480	−0.22	AAM96
	4400	−1.56	…	−1.20	Gizis97
G65-22	5000	−1.66	4971	−1.75	AAM96
	5000	−1.66	4982	−1.72	CLLA94
G239-12	5800	−2.62	6025	−2.56	CLLA94
HIP 70152	4800	−0.05	…	0.22	RN91
	4800	−0.05	…	−0.03	Reid01
HIP 74235	4900	−1.51	5040	−1.54	TL99
	4900	−1.51	…	−1.31	TI99
	4900	−1.51	4957	−1.57	CLLA94
	4900	−1.51	4974	−1.52	AAM96
	4900	−1.51	4850	−1.40	Fulbright00
BD +2°2944	6000	−0.02	6036	−0.13	AAM99
G17-25	4950	−1.46	5175	−1.10	Fulbright00
	4950	−1.46	…	−1.08	TI99
	4950	−1.46	5180	−1.35	TL99
	4950	−1.46	4966	−1.34	AAM96
	4950	−1.46	4959	−1.54	CLLA94
LP 445-55	5200	−1.80	…	−1.55	RN91
LP 447-2	5800	−1.79	…	−1.74	RN91
LP 747-18	5800	−0.95	…	−1.22	RN91
G19-25	4900	−2.01	…	−2.03	RN91
	4900	−2.01	4938	−1.88	CLLA94
	4900	−2.01	4977	−1.52	AAM96
BD −8°4501	5800	−1.80	5657	−1.99	CLLA94
	5800	−1.80	5682	−2.79	AAM96
G204-47	5200	−0.88	5249	−0.86	CLLA94
BD +5°3640	4950	−1.34	5080	−1.27	TL99
	4950	−1.34	5012	−1.36	CLLA94
	4950	−1.34	4980	−1.44	AAM96
	4950	−1.34	…	−0.37	RN91
G227-44	5400	−1.45	5501	−1.41	CLLA94
G207-23	5000	−1.90	…	−1.00	RWMRKM01
HD 181007	4700	−1.93	4582	−2.27	AAM96[a]
LP 752-18	5800	−1.00	…	−1.73	RN91
LP 753-29	5400	−1.88	…	−2.10	RN91
G23-14	5000	−1.51	5100	−1.40	Carney97
	5000	−1.51	4893	−2.20	CLLA94
LP 815-43	6400	−2.70	6379	−2.64	TI99
	6400	−2.70	6500	−2.95	PMBH00
BD +22°4567	4800	−0.33	…	−0.22	Eggen98
HIP 109801	4600	−1.70	4661	−1.43	CLLA94
	4600	−1.70	…	−0.92	RN91
Ross 237	4900	−1.49	4947	−1.38	CLLA94
BD +28°4634	5000	−0.30	…	−0.15	SPC93

NOTE.—The following references were based on spectroscopic data: Beers99, CLLA94, Carney97, Clementini99, Fulbright00, Gizis97, Primas00, RN91, TI99, and TL99.

[a] Giant star assumed to be a dwarf.

REFERENCES.—AAM96 = Alonso et al. 1996a; AAM99 = Alonso et al. 1999a; Beers99 = Beers et al. 1999; CLLA94 = Carney et al. 1994; Carney97 = Carney et al. 1997; Clementini99 = Clementini et al. 1999; Eggen87 = Eggen 1987; Eggen98 = Eggen 1998; Fulbright00 = Fulbright 2000; GL00 = Gay & Lambert 2000; Gizis97 = Gizis 1997; Morrison01 = Morrison et al. 2001; Norris86 = Norris 1986; Primas00 = Primas et al. 2000; Reid01 = Reid et al. 2001; RN91 = Ryan & Norris 1991; SPC93 = Schuster, Parrao, & Contreras Martinez 1993; TI99 = Thévenin & Idiart 1999; TL99 = Tomkin & Lambert 1999.

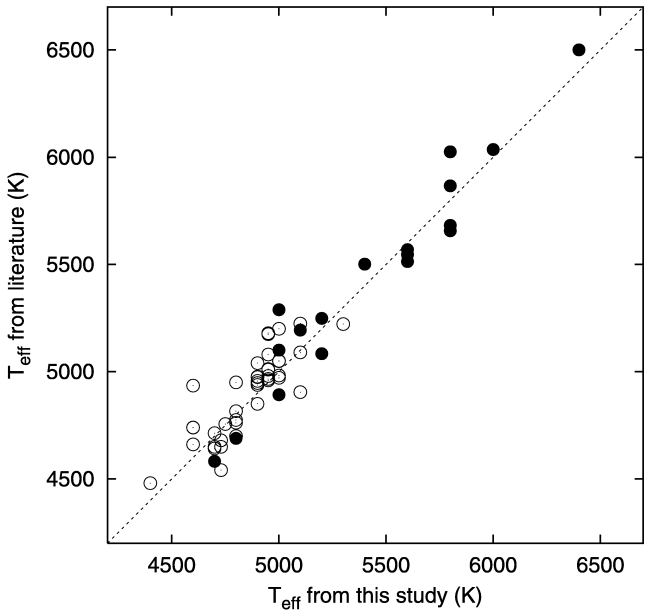

FIG. 5.—T_{eff} comparisons between this work and various literature studies. The filled circles represent stars that have neither MgH nor TiO bands in their spectra. The dotted line represents the line of equality.

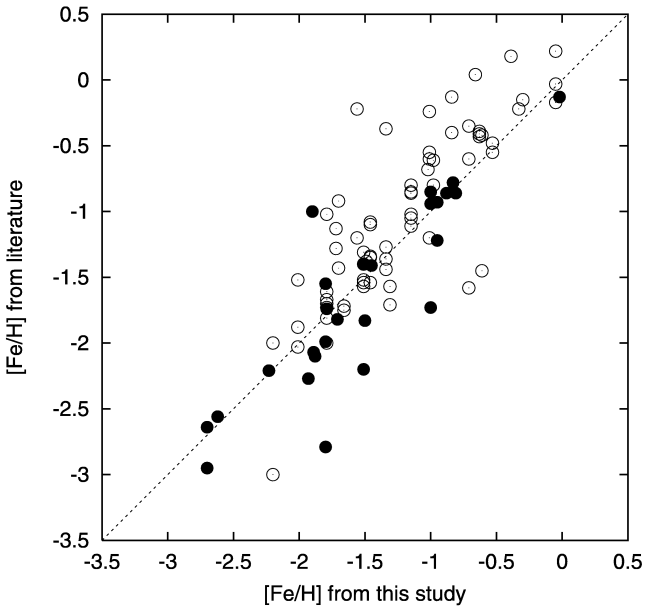

FIG. 6.—[Fe/H] comparisons between this work and various literature studies. The filled circles represent stars that have neither MgH nor TiO bands in their spectra. The dotted line represents the line of equality. We note that the scatter for the open circles is slightly larger than for the filled circles.

requires a metallicity and gravity estimate. The derived T_{eff} are insensitive to the input metallicity and gravity. We also computed T_{eff} derived by use of the T_{eff} : [Fe/H] : color relations given in Alonso et al. (1996b, 1999b) assuming values for [Fe/H] from this study (see Table 3).

MgH and TiO bands will not be visible in the spectra of stars with sufficiently high temperatures and/or low abundances. Indeed, this is the case for 34 of the stars as noted in the last column of Table 1.

5. DISCUSSION

5.1. Kinematics

We selected stars with large reduced proper motions and therefore expect the observed sample to be kinematically distinct from the thin disk. Following the prescription given by Johnson & Soderblom (1987), the Galactic space-velocity components *U*, *V*, and *W* were calculated along with the associated uncertainties (see Table 1). To correct for the solar motion with respect to the LSR, we assumed the Dehnen & Binney (1998) values (-10, $+5$, $+7$) km s^{-1} in (*U*, *V*, *W*). In the absence of *Hipparcos* parallaxes, spectroscopic parallaxes were determined by using the derived model parameters and the Girardi et al. (2000) isochrones. Figure 7 shows [Fe/H] versus U_{LSR}, V_{LSR}, and W_{LSR}. We identify stars that lag the LSR, $V < -50$ km s^{-1}, as being members of the thick disk or halo. As expected from a reduced proper-motion constraint, we have selected stars that belong to populations kinematically distinct from the thin disk. Many of the observed stars have abundances indicative of the thick disk and halo. Ryan (1989) claimed that the NLTT catalog was a rich source of subdwarfs as identified by the ultraviolet excess. Figure 8 shows the numbers of stars for various metallicity bins. Given that 27 stars have [Fe/H] ≤ -1.5, our data endorse Ryan's claims. From the kinematics and abundances of the observed stars, we conclude that the reduced proper-motion constraint successfully selected metal-weak thick-disk and halo stars.

5.2. Temperature

Our goal was to find cool stars, 4000 K $< T_{eff} <$ 4700 K. Of the 134 stars presented in this paper, 44 had $T_{eff} \leq 4700$ K and, given the uncertainties in T_{eff}, we note that 69 of the 134 stars had $T_{eff} \leq 4800$ K. Figure 9 shows the number of stars versus T_{eff} for this study and the Carney et al. (1994) study. Our sample includes cooler stars than the Carney study, which highlights the different temperature regimes of interest. In addition to the stars presented here, we have observations of a further 100 stars, which are simply too cool for equivalent width analysis. Molecular bands make identification of the continuum virtually impossible, and finding unblended Fe I and Fe II lines is problematic. Given the strength of the TiO bands, we assume that these stars are all cooler than 4500 K. We are exploring various techniques for determination of the stellar parameters. The strength of the TiO bandheads in some stars suggests rather low values for T_{eff}, thus we reconfirm Ryan's finding regarding Luyten's photometry that "the values tabulated in the NLTT catalog must be regarded as approximate only."

TABLE 3
COMPARISON OF $T_{\rm eff}$

Star	This Study $T_{\rm eff}$ (K)	This Study [Fe/H]	Color Index	$T_{\rm eff}$ from Color Relation (K)
PLX 5805	4600	−1.72	$B-V$	4764
	4600	−1.72	$J-K$	4464
BD −14°142	6200	−1.21	$B-V$	5113
	6200	−1.21	$V-K$	6327
	6200	−1.21	$J-K$	5860
LP 646-24	4800	−1.01	$V-K$	4666
	4800	−1.01	$J-K$	4665
G72-34	4800	−2.23	$J-K$	4654
BD −4°290	4900	−0.01	$B-V$	4544
BD +8°335	5100	−0.98	$B-V$	4485
HIP 10412	4600	−0.40	$B-V$	4491
Cool 340	4800	−0.40	$B-V$	4581
	4800	−0.40	$V-K$	4158
	4800	−0.40	$J-K$	4544
BD +4°415	4750	−0.63	AAM96[a]	4756
GJ 1064A	5000	−1.15	$B-V$	4717
	5000	−1.15	$V-K$	4963
	5000	−1.15	$J-K$	4978
GJ 1064B	4800	−1.15	$B-V$	4692
	4800	−1.15	$V-K$	4591
	4800	−1.15	$J-K$	5791
BD −4°680	5800	−1.89	AAM96[a]	5866
G39-36	4200	−2.50	$J-K$	4400
G81-41	4550	−0.96	$B-V$	4357
BD −10°1085	5100	−0.50	$B-V$	4676
	5100	−0.50	$V-K$	4982
	5100	−0.50	$J-K$	4978
BD +19°869	4600	−1.01	$V-K$	4245
	4600	−1.01	$J-K$	4287
PLX 1219	4600	−1.79	AAM96[a]	4739
HIP 27928	4200	−0.93	$J-K$	4082
G103-27	5600	−0.95	$B-V$	5580
	5600	−0.95	$V-K$	5118
	5600	−0.95	$J-K$	5153
G101-34	5000	−1.50	$B-V$	4724[b]
G103-50	4700	−2.20	AAM96[a]	4713
HIP 30567	4700	−0.60	$B-V$	4701
AC +78°2199	5000	−0.03	$B-V$	4408
	5000	−0.03	$V-K$	5036
	5000	−0.03	$J-K$	5026
G88-1	4600	−0.84	$B-V$	4700
	4600	−0.84	$V-K$	4394
	4600	−0.84	$J-K$	4482
BD −17°1716	4600	−0.08	$B-V$	4438
	4600	−0.08	$V-K$	4397
	4600	−0.08	$J-K$	4301
G87-27	5100	−0.61	$B-V$	4697[b]
G87-35	5300	−0.53	$B-V$	6191
	5300	−0.53	$V-K$	5055
	5300	−0.53	$J-K$	5242
G193-49	5000	−0.39	$B-V$	4538
G90-4	5600	−0.81	$b-y$, c1	5473
LP 208-60	5800	−0.22	$J-K$	5121
G115-1	4800	−1.33	$B-V$	4407
	4800	−1.33	$V-K$	4884
	4800	−1.33	$J-K$	4784
PLX 2019	4600	−1.72	AAM96[a]	4740
LP 209-14	5400	−1.36	$J-K$	5701
G9-31	5600	−1.00	AAM96[a]	5569
LP 36-78	5150	0.25	$B-V$	4786
LP 786-61	5800	−0.76	$B-V$	5557
Ross 94	4600	0.00	$B-V$	3652[b]
	4600	0.00	$V-K$	3744[b]
	4600	0.00	$J-K$	4207[b]
G116-55	5600	−2.10	$B-V$	5513
	5600	−2.10	$V-K$	5740
	5600	−2.10	$J-K$	5486
G43-7	4950	−1.02	$B-V$	6627
G161-84	4700	−1.31	$J-K$	4471
LP 788-55	4700	−0.53	$J-K$	4612
Wolf 334	5200	−1.71	$J-K$	5455
LP 315-12	5100	−0.98	$V-K$	4582
	5100	−0.98	$J-K$	4756
LP 429-17	4750	−0.10	$B-V$	4658
	4750	−0.10	$V-K$	4563
	4750	−0.10	$J-K$	4604
BD +12°2201	4500	−0.23	$V-K$	4245
	4500	−0.23	$J-K$	4095
LP 790-19	4300	−0.51	$J-K$	4119
BD −9°3104	4900	−0.60	$B-V$	4853
	4900	−0.60	$V-K$	4785
	4900	−0.60	$J-K$	4884
G119-21	4600	−0.48	$B-V$	4126
	4600	−0.48	$V-K$	4304
	4600	−0.48	$J-K$	4604
BD +31°2175	4800	−0.17	$B-V$	4502
	4800	−0.17	$V-K$	4826
	4800	−0.17	$J-K$	4673
PLX 2529.1	4800	−0.58	$B-V$	4610
	4800	−0.58	$V-K$	4653
	4800	−0.58	$J-K$	4650
G119-45	4800	0.14	$J-K$	4537
G58-36	4600	−0.05	$J-K$	4540
G253-46	5200	−0.57	$V-K$	5300
	5200	−0.57	$J-K$	5394
HIP 55128	4900	−0.38	$B-V$	4609
	4900	−0.38	$V-K$	4685
	4900	−0.38	$J-K$	4728
LP 792-12	4800	−0.39	$B-V$	4261
G122-22	4400	−1.36	$V-K$	4465
G163-80	4700	0.05	$J-K$	4658
Ross 109	5300	−1.53	$B-V$	5610
LP 733-14	4700	−0.57	$V-K$	4534
	4700	−0.57	$J-K$	4407
Wolf 1424	4600	−1.19	$V-K$	4491
	4600	−1.19	$J-K$	4358
LP 734-101	5500	0.06	$B-V$	5548
G13-29	4800	−0.66	$V-K$	4684
	4800	−0.66	$J-K$	4338
G198-61	5300	−0.12	$B-V$	5147
	5300	−0.12	$V-K$	5139
	5300	−0.12	$J-K$	5460
G149-9	4900	−0.62	$V-K$	4731
	4900	−0.62	$J-K$	4631

TABLE 3 (*Continued*)

Star	This Study $T_{\rm eff}$ (K)	This Study [Fe/H]	Color Index	$T_{\rm eff}$ from Color Relation (K)
HIP 62627	4800	−0.24	$B-V$	4295
G149-18	5000	−0.03	$B-V$	4206
	5000	−0.03	$V-K$	4643
	5000	−0.03	$J-K$	4650
HD 114095	4730	−0.71	$B-V$	4422[b]
	4730	−0.71	$V-K$	4510[b]
	4730	−0.71	$J-K$	4565[b]
	4730	−0.71	AAM96[a]	4541[c]
BD +68°714	4900	−0.05	$B-V$	4424
	4900	−0.05	$V-K$	4797
	4900	−0.05	$J-K$	4952
Ross 466	5000	−0.86	$J-K$	4784
LHS 2715	4400	−1.56	AAM96[a]	4480
G65-22	5000	−1.66	AAM96[a]	4971
LP 172-89	4800	−0.49	$B-V$	4384
LP 738-45	4400	−0.12	$J-K$	4264
G255-44	4900	−1.30	$B-V$	4901
	4900	−1.30	$V-K$	4686
	4900	−1.30	$J-K$	4813
BD +30°2490	4600	−0.18	$B-V$	4005
	4600	−0.18	$V-K$	4185
	4600	−0.18	$J-K$	4442
G239-12	5800	−2.62	$B-V$	5460
HIP 70152	4800	−0.05	$B-V$	4446
LP 500-92	4500	−0.38	$B-V$	3765
	4500	−0.38	$V-K$	4184
	4500	−0.38	$J-K$	4294
LP 175-8	4900	−0.31	$B-V$	4490
	4900	−0.31	$V-K$	4678
	4900	−0.31	$J-K$	4842
HD 131287	4800	−0.04	$B-V$	5715
LP 502-8	5000	−0.95	$B-V$	4559
HIP 74235	4900	−1.51	AAM96[a]	4971
BD +2°2944	6000	−0.02	AAM99[a]	5856[b]
G225-50	4600	−0.13	$B-V$	3964
	4600	−0.13	$V-K$	4637
	4600	−0.13	$J-K$	4341
LP 330-7	4800	−0.22	$B-V$	4087
	4800	−0.22	$V-K$	4743
	4800	−0.22	$J-K$	4708
G202-57	4900	−1.05	$B-V$	4917
	4900	−1.05	$V-K$	4617
	4900	−1.05	$J-K$	4612
G17-25	4950	−1.46	AAM96[a]	4966
BD −14°4454	4600	−0.95	$V-K$	4474
	4600	−0.95	$J-K$	4334
LP 445-55	5200	−1.80	$V-K$	5807
	5200	−1.80	$J-K$	5420
LP 447-2	5800	−1.79	$B-V$	5404
	5800	−1.79	$V-K$	5611
	5800	−1.79	$J-K$	5491
LP 747-18	5800	−0.95	$B-V$	5380
	5800	−0.95	$V-K$	4827
	5800	−0.95	$J-K$	5103
LP 447-34	4800	−0.35	$B-V$	5136
	4800	−0.35	$V-K$	4699
	4800	−0.35	$J-K$	4760
G19-25	4900	−2.01	AAM96[a]	4977
BD −8°4501	5800	−1.80	AAM96[a]	5682
G204-47	5200	−0.88	$B-V$	4923
	5200	−0.88	$V-K$	5044
	5200	−0.88	$J-K$	5394
BD +5°3640	4950	−1.34	AAM96[a]	4980
BD −17°5287	5800	−0.70	$B-V$	4584
G227-44	5400	−1.45	$B-V$	4932
G207-23	5000	−1.90	$B-V$	4798
	5000	−1.90	$V-K$	5279
	5000	−1.90	$J-K$	5176
HD 181007	4700	−1.93	$B-V$	4659[b]
	4700	−1.93	$V-K$	4676[b]
	4700	−1.93	$J-K$	4887[b]
LP 752-18	5800	−1.00	$B-V$	6055
G23-14	5000	−1.51	$b-y$	4958[b]
LP 575-39	4700	−0.42	$B-V$	4100
LP 575-40	4800	−0.10	$B-V$	4349
LP 815-43	6400	−2.70	$B-V$	5193
	6400	−2.70	$V-K$	6509
	6400	−2.70	$J-K$	5973
HD 200968	5000	−0.16	$B-V$	4550
BD +22°4567	4800	−0.33	$B-V$	4315
BD +30°4633	4600	−0.01	$B-V$	3889
HIP 109801	4600	−1.70	$J-K$	4593
Ross 237	4900	−1.49	$B-V$	5410
	4900	−1.49	$V-K$	4590
	4900	−1.49	$J-K$	4879
Ross 242	4700	−0.94	$B-V$	4680
	4700	−0.94	$V-K$	4682
	4700	−0.94	$J-K$	4646
LP 702-79	4800	0.05	$V-K$	4605
	4800	0.05	$J-K$	4331
HIP 115664	4600	−0.90	$V-K$	4370
	4600	−0.90	$J-K$	4411
BD +28°4634	5000	−0.30	$B-V$	4515
	5000	−0.30	$V-K$	4825
	5000	−0.30	$J-K$	4712

NOTE.—Comparison of $T_{\rm eff}$ derived in this study with $T_{\rm eff}$ calculated from Alonso et al. 1996b. Photometry from the following sources: B and V taken from the Guide Star Catalog II, J and K taken from the Two Micron All Sky Survey (2MASS; Skrutskie et al. 1997), and $b-y$ and c1 taken from Schuster et al. 1993.

[a] $T_{\rm eff}$ determined from direct application of the IRFM.

[b] Giant star; $T_{\rm eff}$ derived from Alonso et al. 1999b relation.

[c] Giant star assumed to be a dwarf.

REFERENCES.—AAM96 = Alonso et al. 1996a; AAM99 = Alonso et al. 1999a.

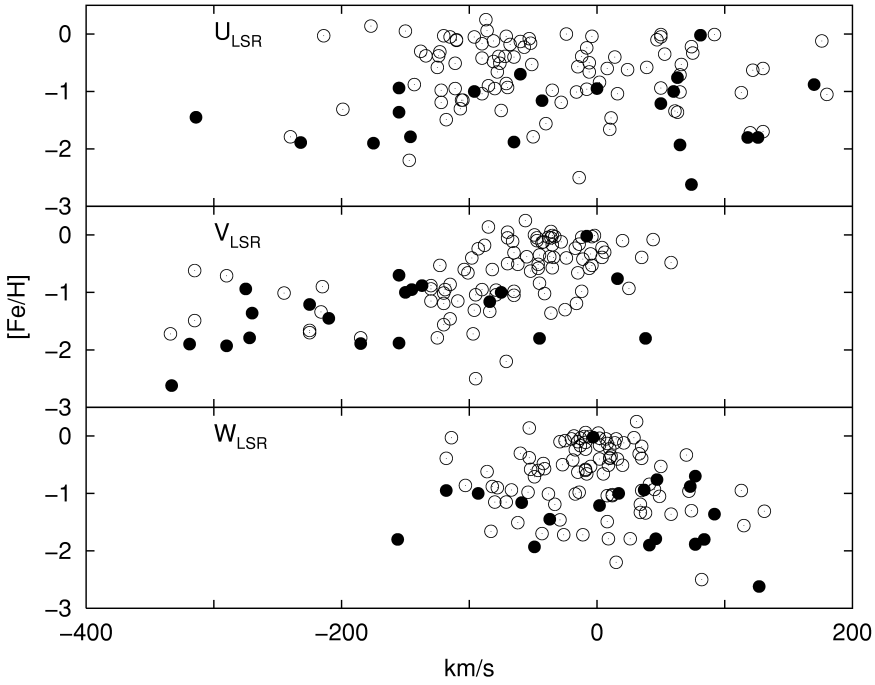

FIG. 7.—Galactic space-velocity *U*, *V*, and *W* vs. [Fe/H], where *U*, *V*, and *W* are relative to the LSR. Filled circles represent stars that have neither MgH nor TiO bands in their spectra. Only stars that have $(\sigma_U + \sigma_V + \sigma_W) / (|U| + |V| + |W|) < 0.7$ are shown, 117 out of 134. A considerable fraction of the sample noticeably lag the LSR ($V < -50$ km s^{-1}).

5.3. Metallicity

Figure 8 shows the number of stars versus metallicity for this study, the Carney et al. (1994) sample, and the Ryan & Norris (1991) sample. It is clear that our sample is considerably smaller than the Ryan and Carney studies. The distributions are similar between the Carney sample and our study, which is rather interesting. Our complete list of NLTT candidates comprised 4445 stars of which we observed some 230 stars. We derived stellar parameters for 134 stars and found 27 with [Fe/H] ≤ -1.50, with several having prior metallicity estimates. Presumably, if we were to observe the remaining 4000+ candidates, we would find ~500 stars with [Fe/H] ≤ -1.50. The distribution of the Ryan sample differs from this study and from the Carney study. The Ryan sample peaks at a lower metallicity where this is simply a selection effect. The original Ryan (1989) sample provided broadband photometry where metal-poor candidates were identified by the ultraviolet excess. The stars reobserved in Ryan & Norris (1991) were those stars identified in Ryan (1989) as having an ultraviolet excess corresponding to [Fe/H] < -1.2, that is, $\delta(U-B)_{0.6} > 0.2$.

For the 27 stars we observed with [Fe/H] ≤ -1.50, there were 11 sufficiently cool to provide MgH features. These were the cool subdwarfs with molecular features that we were interested in finding. Again, if were to observe the remaining 4000+ NLTT candidates, there would presumably be ~200 such objects.

In our sample, the lack of cool subdwarfs with [Fe/H] ≤ -2 could be attributed to two reasons. First, the volume we are sampling may not be large enough, and second, our ability to identify genuine subdwarfs may be inefficient. Regarding the volume we are sampling, according to the Girardi et al. (2000) isochrones, for stars with $T_{\rm eff} = 4500$ K and [Fe/H] $= -1.68$, our $m_R \simeq V = 13$ limit corresponds to a maximum distance of merely ~75 pc. This volume further decreases when we consider even more metal poor stars. More importantly, applying our magnitude limit to a star with $T_{\rm eff} = 5500$ K and [Fe/H] $= -1.68$ corresponds to a maximum distance of ~220 pc. This represents a volume 27 times larger than for our cooler targets. Carney et al. (1994) considered stars as faint as $V = 16$, which, combined with the intrinsic brightness of warmer targets, results in a considerably larger volume. Obviously the number of cool metal-poor stars in a particular volume increases as the volume increases. Regarding the efficiency of identifying candidate subdwarfs, recent work by Salim & Gould (2002) provides more accurate $V-J$ photometry for NLTT stars based on 2MASS infrared photometry and USNO-A optical photometry. Combining the precise photometry with the proper motions generates a reduced proper-motion diagram with well-defined white dwarf, subdwarf, and disk dwarf populations. From this revised NLTT catalog and proper-motion diagram, we expect that these subdwarf candidates will contain a considerably higher fraction of genuine subdwarfs than our original list of

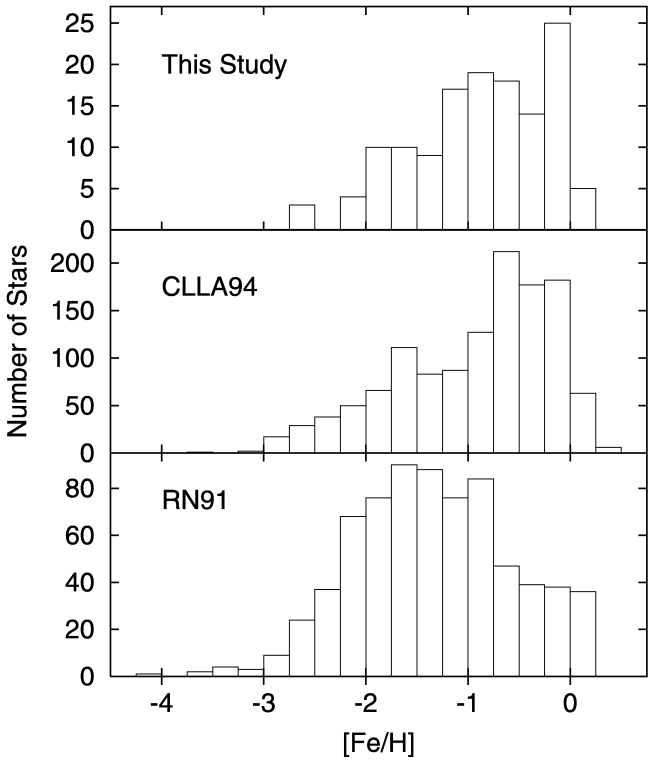

FIG. 8.—Number of stars vs. metallicity for this study (*top panel*), the Carney et al. (1994) study (*middle panel*), and the Ryan & Norris (1991) study (*bottom panel*). Note the similar distributions between this study and the Carney work. The Ryan distribution peaks at a lower metallicity since their sample consists of stars identified as having an ultraviolet excess corresponding to [Fe/H] < -1.2.

candidates. Observations of candidate subdwarfs selected from the Salim & Gould (2002) $V-J$ reduced proper-motion diagram will be made.

Alternatively, we could consider what volume is needed to obtain a large number of stars with $-3 <$ [Fe/H] < -2 and 4000 K $< T_{\rm eff} <$ 4500 K. Our observed NLTT candidates provided just one star within the desired range of parameters, G39-36 ($T_{\rm eff}$ = 4200 K, [Fe/H] = -2.5). From the Yi et al. (2001) isochrones, we estimate that G39-36 lies at a distance of 27 pc from the Sun. Given the stellar parameters of G39-36, our $V = 13$ magnitude limit represents a maximum volume of merely 36 pc. Since we observed around 200 of the 4445 NLTT candidates, perhaps there are 10–20 cool subdwarfs among our list of NLTT candidates. If we conservatively estimate that there are five cool subdwarfs ($-3 <$ [Fe/H] < -2, 4000 K $< T_{\rm eff} <$ 4500 K) within a radius of 50 pc around the Sun, then we expect around 300 cool subdwarfs within a radius of 200 pc. A search for subdwarfs similar to G39-36 out to a distance of 200 pc would require a magnitude limit of $V \simeq 17$. Such a limit implies a low-resolution, low-S/N search technique or a photometric search to weed out the intruders.

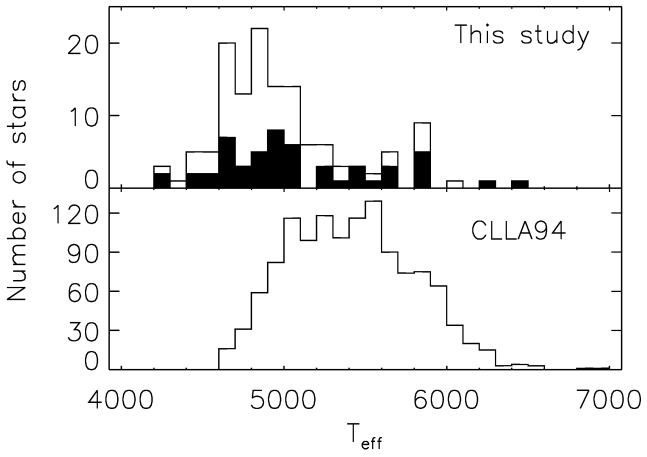

FIG. 9.—Number of stars vs. $T_{\rm eff}$ for this study (*top panel*) and the Carney et al. (1994) study (*bottom panel*). In the top panel, the filled histogram represents the distribution of stars with [Fe/H] ≤ -1.0. The distribution for our sample peaks at lower values of $T_{\rm eff}$ than the Carney sample. This was expected since we deliberately selected cooler color classes.

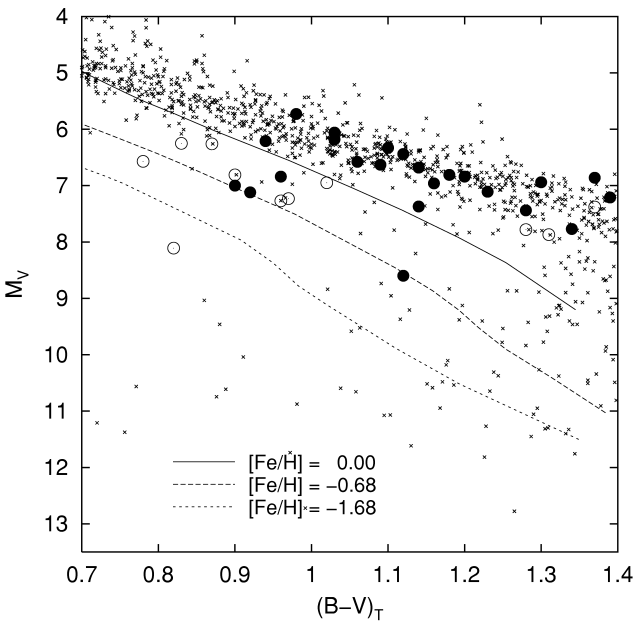

FIG. 10.—M_V, $(B-V)_{\rm T}$ color-magnitude diagram with crosses marking *Hipparcos* stars with $\sigma_\pi/\pi < 15$ and $\pi > 32$ mas. Closed circles represent observed stars with [Fe/H] ≥ -1.0, while open circles represent [Fe/H] < -1.0. Girardi et al. (2000) isochrones using Johnson $(B-V)$ for [Fe/H] = 0.0, -0.68, -1.68 are overplotted. $(B-V)_{\rm T}$ is increasingly redder than the Johnson $(B-V)$ as the stars get cooler, as noted by Reid et al. (2001).

5.4. *Hipparcos*

Having observed a number of cool stars contained in the *Hipparcos* catalog, we can comment upon the results of Reid et al. (2001). The majority of *Hipparcos* stars were selected by their large reduced proper motion from the NLTT catalog rather than the position in the color-magnitude diagram. Reid et al. (2001) claimed that in a color-magnitude diagram produced from *Hipparcos* parallaxes, the majority of stars with $(B-V) \leq 0.8$ situated below the solar-metallicity main sequence were incorrectly positioned as a result of errors in the colors. These stars, located where subdwarfs ought to lie, were metal-rich disk dwarfs rather than subdwarfs. Reid et al. (2001) also showed that the Tycho colors $(B-V)_T$ are redder than the Johnson $(B-V)$ colors. In Figure 10, we take the Tycho colors and *Hipparcos* parallaxes to produce a color-magnitude diagram overlaying the stars we observed. Nearby stars ($\pi > 32$ mas) with accurate parallaxes ($\sigma_\pi/\pi < 0.15$) are included to represent the disk population, [Fe/H] $\simeq 0$. Our few observations confirm and extend the Reid et al. (2001) findings in the regime $0.8 < B-V < 1.4$. Metal-poor stars with [Fe/H] < -1.0 are located among disk stars. Also, metal-rich stars with [Fe/H] > -1.0 are offset from the disk main sequence. The effect of the redder Tycho colors is evident as the disk main sequence is systematically offset from the Girardi et al. (2000) [Fe/H] $= 0$ isochrone. We intend to observe additional *Hipparcos* subdwarf candidates in the range $0.8 < (B-V)_T < 1.2$ not only to find cool subdwarfs but to further test the findings made by Reid et al. (2001).

6. CONCLUDING REMARKS

We present stellar parameters for 134 candidate subdwarfs selected by their reduced proper motion, offset from the solar-metallicity main sequence, or from the literature. Our goal was to provide a large database of cool subdwarfs. Our selection criteria were successful in identifying cool stars (69 with $T_{\rm eff} <$ 4800 K) and metal-poor stars (27 with [Fe/H] ≤ -1.50). Of our sample, 11 stars were sufficiently cool to provide measurable MgH lines with [Fe/H] < -1.50. Armed with a sample of cool subdwarfs, we can begin to exploit their unique qualities. For a subset of our sample, we have measured the Mg isotopic abundance ratios and compared the observed trends with predictions from models of Galactic chemical evolution. This work will be presented in a future paper. We also intend to make further observations of candidate subdwarfs. Targets will be selected from the revised NLTT catalog (Salim & Gould 2002). Cool *Hipparcos* subdwarf candidates will be observed, and we anticipate that Christlieb and collaborators will identify cool subdwarfs in the Hamburg/ESO survey data.

We thank George Preston for helpful comments and the staff of the Hobby-Eberly telescope for service observations of our targets. We acknowledge support via the grant F-634 from the Robert A. Welch Foundation of Houston, Texas. This research has made use of the SIMBAD database, operated at CDS, Strasbourg, France, and NASA's Astrophysics Data System.

REFERENCES

Alibés, A., Labay, J., & Canal, R. 2001, A&A, 370, 1103
Alonso, A., Arribas, S., & Martínez-Roger, C. 1996a, A&AS, 117, 227
———. 1996b, A&A, 313, 873
———. 1999a, A&AS, 139, 335
———. 1999b, A&AS, 140, 261
Beers, T. C., Preston, G. W., & Shectman, S. A. 1985, AJ, 90, 2089
———. 1992, AJ, 103, 1987
Beers, T. C., Rossi, S., Norris, J. E., Ryan, S. G., & Shefler, T. 1999, AJ, 117, 981
Bond, H. E. 1970, ApJS, 22, 117
———. 1980, ApJS, 44, 517
Carney, B. W., & Latham, D. W. 1987, AJ, 93, 116
Carney, B. W., Latham, D. W., Laird, J. B., & Aguilar, L. A. 1994, AJ, 107, 2240
Carney, B. W., Wright, J. S., Sneden, C., Laird, J. B., Aguilar, L. A., & Latham, D. W. 1997, AJ, 114, 363
Christlieb, N. 2000, Ph.D. thesis, Univ. Hamburg
Clementini, G., Gratton, R. G., Carretta, E., & Sneden, C. 1999, MNRAS, 302, 22
Dehnen, W., & Binney, J. J. 1998, MNRAS, 298, 387
Edvardsson, B., Andersen, J., Gustafsson, B., Lambert, D. L., Nissen, P. E., & Tomkin, J. 1993, A&A, 275, 101
Eggen, O. J. 1987, AJ, 93, 393
———. 1998, AJ, 115, 2397
ESA. 1997, The *Hipparcos* and Tycho Catalogues, VizieR Online Data Catalog
Fuchs, B., & Jahreiß, H. 1998, A&A, 329, 81
Fulbright, J. P. 2000, AJ, 120, 1841
Gay, P. L., & Lambert, D. L. 2000, ApJ, 533, 260
Girardi, L., Bressan, A., Bertelli, G., & Chiosi, C. 2000, A&AS, 141, 371
Gizis, J. E. 1997, AJ, 113, 806
Goswami, A., & Prantzos, N. 2000, A&A, 359, 191
Grevesse, N., & Sauval, A. J. 1999, A&A, 347, 348
Harlow, J. J. B., Ramsey, L. W., Andersen, D. R., Fleig, J. D., Rhoads, B. T., & Engel, L. G. 1996, BAAS, 28, 1324
Hauschildt, P. H., Allard, F., & Baron, E. 1999, ApJ, 512, 377
Johnson, D. R. H., & Soderblom, D. R. 1987, AJ, 93, 864
Kurucz, R. 1993, Kurucz CD-ROM 13, ATLAS9 Stellar Atmosphere Programs and 2 km/s Grid (Cambridge: Smithsonian Astrophys. Obs.), 13
Lambert, D. L., Heath, J. E., Lemke, M., & Drake, J. 1996, ApJS, 103, 183
Luyten, W. J. 1979, New Luyten Catalogue of Stars with Proper Motions Larger than Two Tenths of an Arcsecond, Vols. 1–4 (Minneapolis: Univ. Minnesota)
———. 1980, New Luyten Catalogue of Stars with Proper Motions Larger than Two Tenths of an Arcsecond, Vols. 1–4 (Minneapolis: Univ. Minnesota)

Luyten, W. J., & Hughes, H. S. 1980, Proper Motion Survey with the Forty-Eight Inch Schmidt Telescope. LV. First Supplement to the NLTT Catalogue (Minneapolis: Univ. Minnesota)
McWilliam, A., Preston, G. W., Sneden, C., & Searle, L. 1995, AJ, 109, 2757
Morrison, H. L., Olszewski, E. W., Mateo, M., Norris, J. E., Harding, P., Dohm-Palmer, R. C., & Freeman, K. C. 2001, AJ, 121, 283
Norris, J. 1986, ApJS, 61, 667
Primas, F., Molaro, P., Bonifacio, P., & Hill, V. 2000, A&A, 362, 666
Reid, I. N., van Wyk, F., Marang, F., Roberts, G., Kilkenny, D., & Mahoney, S. 2001, MNRAS, 325, 931
Ryan, S. G. 1989, AJ, 98, 1693
Ryan, S. G., & Norris, J. E. 1991, AJ, 101, 1835
Salim, S., & Gould, A. 2002, ApJ, 575, L83
Schuster, W. J., Parrao, L., & Contreras Martinez, M. E. 1993, A&AS, 97, 951
Skrutskie, M. F., et al. 1997, in Astrophysics and Space Science Library 210, The Impact of Large Scale Near-IR Sky Surveys, ed. F. Garzón et al. (Dordrecht: Kluwer), 25
Sneden, C. A. 1973, Ph.D. thesis, Univ. Texas
Thévenin, F., & Idiart, T. P. 1999, ApJ, 521, 753
Timmes, F. X., Woosley, S. E., & Weaver, T. A. 1995, ApJS, 98, 617
Tomkin, J., & Lambert, D. L. 1999, ApJ, 523, 234
Tull, R. G., MacQueen, P. J., Sneden, C., & Lambert, D. L. 1995, PASP, 107, 251
van Altena, W. F., Lee, J. T., & Hoffleit, D. 1995, Yale Trigonometric Parallaxes, VizieR Online Data Catalog
Yi, S., Demarque, P., Kim, Y., Lee, Y., Ree, C. H., Lejeune, T., & Barnes, S. 2001, ApJS, 136, 417